

## ON THE STABILITY OF VERY MASSIVE PRIMORDIAL STARS

I. BARAFFE

Ecole Normale Supérieure, C.R.A.L. (UMR 5574 CNRS), 69364 Lyon Cedex 07, France

A. HEGER AND S. E. WOOSLEY  
Department of Astronomy and Astrophysics  
University of California, Santa Cruz, CA 95064

Draft November 13, 2018

## ABSTRACT

The stability of metal-free very massive stars ( $Z = 0$ ;  $M = 120 - 500 M_{\odot}$ ) is analyzed and compared with metal-enriched stars. Such zero-metal stars are unstable to nuclear-powered radial pulsations on the main sequence, but the growth time scale for these instabilities is much longer than for their metal-rich counterparts. Since they stabilize quickly after evolving off the ZAMS, the pulsation may not have sufficient time to drive appreciable mass loss in  $Z = 0$  stars. For reasonable assumptions regarding the efficiency of converting pulsational energy into mass loss, we find that, even for the larger masses considered, the star may die without losing a large fraction of its mass. We find a transition between the  $\epsilon$ - and  $\kappa$ -mechanisms for pulsational instability at  $Z \sim 2 \times 10^{-4} - 2 \times 10^{-3}$ . For the most metal-rich stars, the  $\kappa$ -mechanism yields much shorter  $e$ -folding times, indicating the presence of a strong instability. We thus stress the fundamental difference of the stability and late stages of evolution between very massive stars born in the early universe and those that might be born today.

*Subject headings:* stars: very massive — stars: pulsations — stars: mass loss — stars: zero metallicity

## 1. INTRODUCTION

The formation and nature of the first generation of so-called Population III (Pop III) stars have been studied and speculated about for over thirty years (Schwarzschild & Spitzer 1953; Yoneyama 1972; Hartquist & Cameron 1977; Palla, Salpeter & Stahler 1983; Silk 1983; and many others), but the extent to which they differed from present day stars in ways other than composition is still debated. Recently, three-dimensional cosmological simulations have reached sufficient resolution on small scales to begin to address the star formation problem (Ostriker & Gnedin 1996; Abel et al. 1998). While considerable uncertainty remains regarding the continued evolution of the dense knots they find in their calculations, these simulations do not exclude the formation of a first generation of quite massive stars  $\sim 100 - 1000 M_{\odot}$  (e.g., Larson 1999; Abel, Bryan, & Norman 2000). Using different numerical methods to analyze the fragmentation of primordial clouds, Bromm et al. (1999) reached similar conclusions. Without further study, especially including the complexity of radiation transport and molecular opacities, it may be premature to conclude that *all* Pop III stars were so massive, but there certainly exists adequate motivation to examine the properties of such stars. In particular, if such massive Pop III stars were ever born, would they retain their large masses until death? That is, would they die as pair-instability supernovae, with possible unique signatures of nucleosynthesis and black hole formation, or would they lose most of their mass and die much the same as present day stars?

It is well known (Ledoux 1941; Schwarzschild & Härm 1959) that, above a critical mass, main sequence stars are vibrationally unstable due to the destabilizing effect of nuclear reactions in their central regions. For stars of Pop I composition, the critical mass for this instability is  $\sim 100 M_{\odot}$  (Schwarzschild & Härm 1959). According to non-linear calculations, such an instability leads to mass loss rather than catastrophic disruption (Appenzeller 1970a; Talbot 1971ab; Papaloizou 1973ab).

Consequently, it has been thought that stars more massive than about  $100 M_{\odot}$  would not survive for long before losing a substantial fraction of their mass. Although the stability of very massive stars has well been explored since the work of Ledoux (1941), somewhat surprisingly, all these analyses have been devoted to solar-like compositions or slightly metal-poor stars (Schwarzschild & Härm 1959; Stothers & Simon 1968; Aizenman et al. 1975; Stothers 1992; Glatzel & Kiriakidis 1993; Kiriakidis et al. 1993), or to helium-core objects such as Wolf-Rayet stars (Maeder 1985; Cox & Cahn 1988). Since the temperature dependence of hydrogen burning and the surface gravitational potential of low metal stars are quite different, it is important to learn whether their stability criteria may also vary.

We have thus performed, to our knowledge, the first stability analysis of zero metallicity stars with  $100 \leq M/M_{\odot} \leq 500$  and have also studied the stability of stars in this mass range for variable initial metal mass fraction  $0 \leq Z \leq 0.02$ . The stellar models are presented in Sect. 2. The results of the linear stability analysis are given in Sect. 3, mass loss estimates are presented in Sect. 4, and our conclusions follow in Sect. 5.

## 2. STELLAR EVOLUTIONARY MODELS

The evolution of four stars of 120, 200, 300 and  $500 M_{\odot}$  was followed from the Zero Age Main Sequence (ZAMS) to the end of core helium burning using an implicit Lagrangian hydrodynamics code adapted to stellar modeling (Langer et al. 1988, Heger 1998; Heger et al. 2000a). Details of the code can be found elsewhere (Heger & Langer 2000), but to summarize the main physics, the opacity is taken from Iglesias and Rogers (1996) and the principal nuclear reaction rates from Caughlan & Fowler (1988) with the rate for  $^{12}\text{C}(\alpha, \gamma)^{16}\text{O}$  multiplied by a constant 1.7 (see also Buchmann 1996). Mass loss is not taken into account, except for what is driven by the pulsations studied here. For zero metallicity stars, radiative mass loss is probably negligible (Kudritzki 2000).

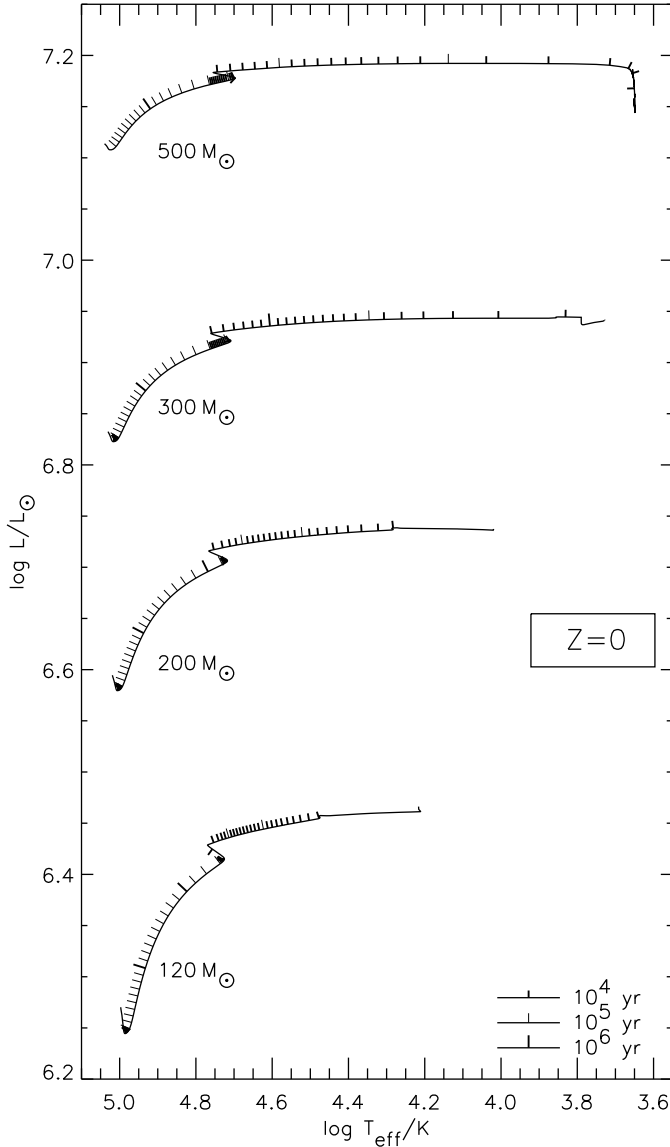


FIG. 1.— Theoretical H-R diagram for stars with  $Z = 0$  and different masses assuming no mass loss. The time-scales of evolution are indicated by marks on the curves.

As was first noted by Ezer and Cameron (1971), massive stars with no metals do not obtain their energy on the main sequence from the pp-cycle as one might naively expect. Instead the star contracts to  $\gtrsim 10^8$  K, burns a trace of helium to carbon, and then expands slightly to burn hydrogen by the CNO cycle. A CNO mass fraction of just a few times  $10^{-9}$  is sufficient to catalyze even the enormous energy generation of such stars. However, owing to this small CNO mass fraction, the star retains a central temperature of  $\sim 10^8$  K throughout central hydrogen burning. As Ezer & Cameron (1971) also noted, these stars are thus much more compact than their metal-enriched counterparts and their radiation, while on the main sequence, is in the ultraviolet (Table 1).

Figure 1 shows the theoretical tracks of our  $Z = 0$  stars in a Hertzsprung-Russell diagram (HRD). All begin to contract dynamically after core helium burning and the star ceases to evolve in the HRD due to shorter evolutionary time-scale of the core compared to the thermal time-scale of the envelope. Note however that, for  $M \gtrsim 300 M_\odot$ , even metal-free stars evolve toward  $T_{\text{eff}} < 10^4$  K and eventually become red supergiants, as

the hydrogen-burning shell becomes more active with increasing stellar mass.

In order to analyze the pulsational stability as a function of metallicity, we repeated our calculations for a wide range of  $Z$  from  $Z = 2 \times 10^{-6}$  to solar,  $Z = 0.02$ , for the  $120 M_\odot$ , and for selected values of  $Z > 0$  for  $M > 120 M_\odot$ . The results are displayed in Fig. 2 for a  $120 M_\odot$  star. Since most of the stability analyses mentioned in Sect. 1 (Ledoux 1941; Schwarzschild & Härm 1959; Appenzeller 1970a; and others) are based upon models with solar metallicity, but computed using only electron scattering opacity, we also calculated, for comparison, models with such an opacity (Fig. 2).

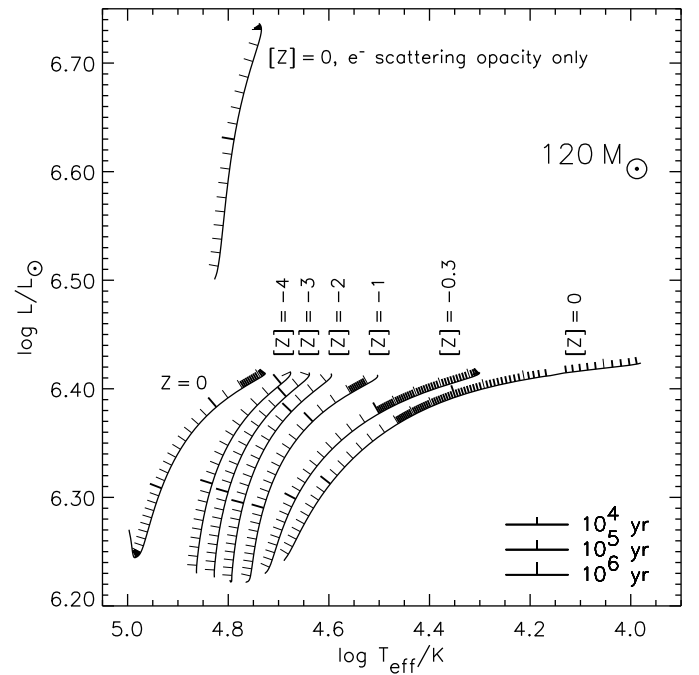


FIG. 2.— Theoretical HR diagram for  $120 M_\odot$  stars with different  $Z$  from hydrogen ignition till 1% of hydrogen left in the center of the star – assuming no mass loss.  $[Z]$  corresponds to  $\log(Z/Z_\odot)$

### 3. LINEAR STABILITY ANALYSIS

A linear non-adiabatic stability analysis of all models was carried out using a radial pulsation code originally developed by Umin Lee (1985; see also Heger et al. 1997; Baraffe et al. 1998; Alibert et al. 1999 for recent applications). The main uncertainty in these calculations is the treatment of convection, which is treated in the “frozen-in” approximation, *i.e.*, the perturbation,  $\delta F_{\text{conv}}$ , of the convective flux is neglected in the linearized energy equation. Although this approximation is an unavoidable consequence of our poor knowledge of the interaction between convection and pulsation, it should not be crucial. As we shall see, the relevant regions for pulsation, which are located in the deep interior of the stars, are fully convective and can be considered as adiabatic. In the outer regions, which may also be important for the pulsation, the convective flux is not the dominant energy transport.

The stability of the fundamental mode and the overtones (up to the fifth overtone) was analyzed starting from ZAMS models up to the end of core helium burning for  $Z = 0$  stars.

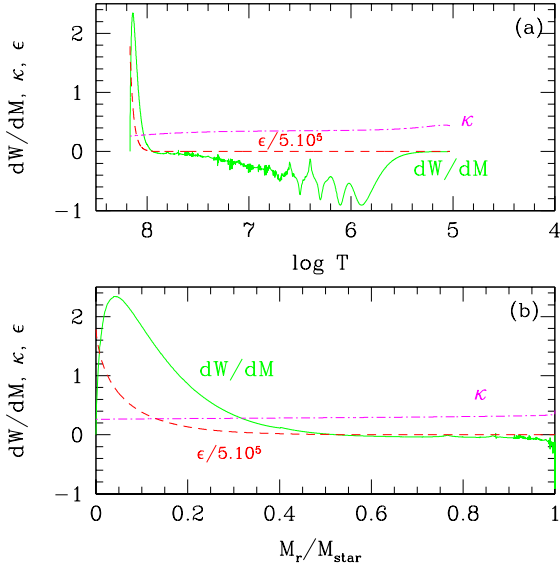


FIG. 3.— (a) Differential work  $dW/dM$ , in arbitrary units, as a function of the temperature ( $T$  in K) in the interior structure of a  $300 M_{\odot}$  with  $Z = 0$ , on the ZAMS. The Rosseland mean opacity  $\kappa$  (in  $\text{cm}^2 \text{g}^{-1}$ ) is indicated by the dash-dotted line. The dashed line corresponds to the nuclear energy generation  $\epsilon$  (in units of  $5 \times 10^5 \text{ erg g}^{-1} \text{ s}^{-1}$ ). (b) Same as (a), but as a function of enclosed mass.

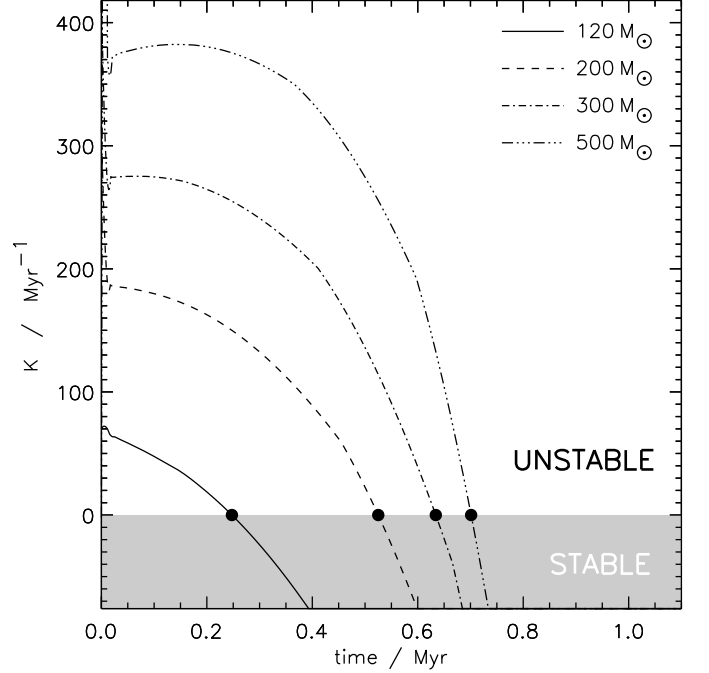


FIG. 4.— Stability coefficient,  $K$ , as a function of time. Positive values indicate growth of the pulsation amplitude while negative values (gray region) correspond to damped oscillations. Shown are  $120 M_{\odot}$  (solid line),  $200 M_{\odot}$  (dashed),  $300 M_{\odot}$  (dash-dotted), and  $500 M_{\odot}$  (dash-triple-dotted) stars of  $Z = 0$  (assuming no mass loss). The filled circles indicate the time where these stars become pulsationally stable.

### 3.1. Metal-free stars

#### 3.1.1. ZAMS models

Table 1 gives, for metal-free ZAMS stars, the effective temperature,  $T_{\text{eff}}$ , stellar radius,  $R$ , central temperature,  $T_c$ , pulsation period,  $P$ , and the pulsational  $e$ -folding time,  $\tau_d$  (Cox 1980). Adopting a time dependence for the eigenfunctions of the form  $\exp(i\sigma t) \exp(Kt)$ , where  $\sigma = 2\pi/P$  is the eigen-frequency and  $K$ , the stability coefficient, the  $e$ -folding time for the growth of the instability is given by  $\tau_d = 1/K$ . For all masses studied, the ZAMS models are unstable and oscillate in the fundamental mode, whereas the overtones are stable. The excitation mechanism is related to the temperature and density dependence of the nuclear energy generation rate near the center of the star, the so-called  $\epsilon$ -mechanism. As was shown by Ledoux (1941), this driving mechanism is efficient because of the large radiation pressure in such massive stars. The driving and damping zones are indicated by correspondingly positive and negative values of  $dW/dM$ , where  $W$  is the work integral (Cox 1980; Unno et al. 1989). This is illustrated in Fig. 3 for the  $300 M_{\odot}$  star. Note that the outer damping regions (see Fig. 3a) give a negligible contribution to the work integral due to the very small amount of mass involved (see Fig. 3b). The same behavior of the work integral is also found for the other masses studied.

#### 3.1.2. Effects of evolution

It is known from previous studies of solar metallicity stars that high mass stars eventually stabilize as they evolve away from the ZAMS (Schwarzschild & Härm 1959; Stothers and Simon 1968; Aizenman et al. 1975; Maeder 1985). Stabilization comes about because of the increase of the mean molecular weight in the inner regions which increases the central condensation (see, e.g., Maeder 1985 for details). The same properties are also found here for metal-free stars. As they evolve away from the ZAMS, their  $e$ -folding time increases, indicating a decrease of the driving term due to nuclear energy compared to the damping term from heat leakage in the envelope. This is a direct consequence of the increase of the central density relative to the mean density. The stars become stable (negative  $K$ ) on the main sequence after a decrease of the central hydrogen mass fraction. This is illustrated in Fig. 4, which displays the stability coefficient,  $K$ , as a function of time for different masses, and in Fig. 5, which shows the time integration of  $K$  during core hydrogen burning. In Fig. 4, the larger value of  $K$  at early times and its rapid variation with time are due to the adjustment of the stellar structure when the initial CNO is produced (see §2). The results are also summarized for the different models in Table 2 which gives the number of  $e$ -foldings,  $A_{\text{max}}$ , by which the amplitude of an initial perturbation would grow in the framework of linear stability analysis, as derived from integration of the stability coefficient with time (see also Fig. 5).

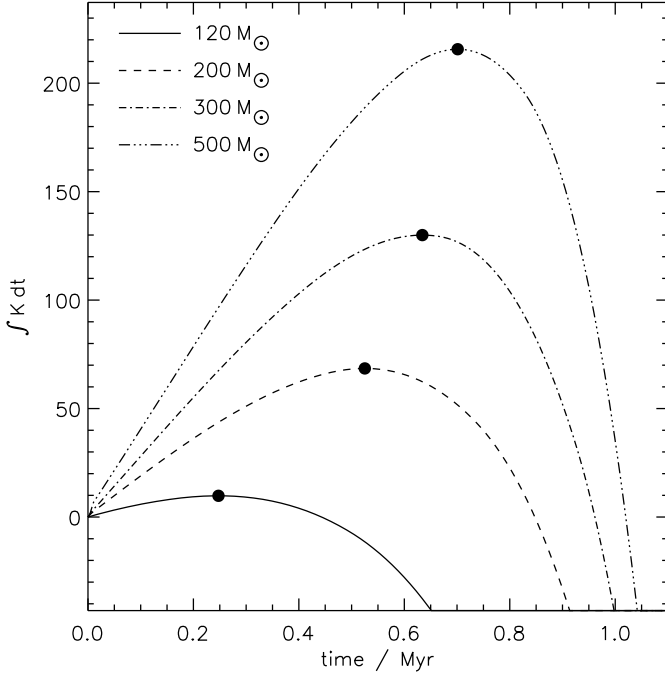


FIG. 5.— Time integration of the stability coefficient,  $K$ . Shown is the integral  $\int_0^t K(t') dt'$  for  $120 M_\odot$  (solid line),  $200 M_\odot$  (dashed),  $300 M_\odot$  (dash-dotted), and  $500 M_\odot$  (dash-triple-dotted) stars of  $Z = 0$  (assuming no mass loss). This gives the number of  $e$ -folds by which an initial pulsation would grow till that time. The filled circles indicate the time where the stars become pulsationally stable. After that the pulsation amplitude is damped quickly. The slope of the curves is shown in Fig. 4.

After reaching pulsational stability during central hydrogen burning, all stars studied remained stable for the rest of central hydrogen burning and most of central helium burning as well. Stars of  $\lesssim 200 M_\odot$  remained stable throughout core helium burning, but stars of initial mass  $\gtrsim 300 M_\odot$  became unstable again towards the end of helium burning. This resurgence of instability happens for a central helium mass fraction  $Y_c = 0.1$  in the  $300 M_\odot$  star and  $Y_c = 0.2$  for the  $500 M_\odot$  star, corresponding to 30 and 50 kyr before the end of central helium burning, respectively. The unstable mode is the fundamental mode, characterized by  $P = 14.2$  d and  $\tau_d = 0.13$  yr for the  $300 M_\odot$  star and  $P = 40$  d and  $\tau_d = 0.16$  yr for  $500 M_\odot$  star. The pulsations in these blue supergiants, with  $T_{\text{eff}} \sim 10^4$  K, exist only in a surface layer that contains very little mass. The  $500 M_\odot$  star, however, expands further and becomes a red supergiant with an extended convective envelope that is characterized by increasing period and decreasing  $e$ -folding time.

The instabilities during core helium burning are characterized by small values of  $\tau_d$  compared to the pulsation period. This indicates the presence of a strong instability that can develop rapidly and reach large amplitudes. Inspection of the work integral shows that the driving zone is located in the hydrogen/helium ionization zone and the excitation mechanism is the standard  $\kappa$ -mechanism.

Note also that the helium cores would quickly become unstable to the  $\epsilon$ -instability, just like their higher metallicity counterparts, if the hydrogen envelope were removed, e.g., to a binary companion.

### 3.2. Effect of $Z$

Table 1 gives the pulsational properties of ZAMS models as a function of  $Z$ . All models analyzed for  $Z > 0$  are vibra-

tionally unstable. The fundamental mode is the pulsation mode and the overtones are stable. Only for  $120 M_\odot$  with  $Z \geq 0.01$ , are both the fundamental (F) and the first overtone (1H) unstable, with an  $e$ -folding time for 1H much shorter than for the F mode. Table 1 also gives the results for solar metallicity models calculated with pure electron scattering opacity. For such models, our results are in good agreement with previous results based on pure electron scattering or on simple opacity laws. Schwarzschild & Härm (1959) find for  $121 M_\odot$ ,  $P = 0.38$  d and  $\tau_d = 1800$  yr, and for  $218 M_\odot$ ,  $P = 0.54$  d and  $\tau_d = 930$  yr. Aizenman et al. (1975) obtain for  $110 M_\odot$ ,  $P = 0.37$  d and  $\tau_d = 644$  yr.

Inspection of Table 1 shows that for a given mass, the period decreases with metallicity. This is a consequence of the smaller radius and more compact structure of metal-poor stars when they reach thermal equilibrium on the ZAMS, a well known effect of  $Z$  on evolutionary models (e.g., Ezer & Cameron 1971; Baraffe & El Eid 1991; Meynet et al 1994). The period,  $P$ , is related to the dynamical time scale of the star,  $P \propto \sqrt{R^3/M}$ . Another important result of Table 1 is the increase of  $\tau_d$  as  $Z$  decreases from  $Z = 0.02$  to 0. This indicates that metal-free stars, although unstable, require a much longer time for the growth of the oscillation amplitudes than solar metallicity stars.

We also note a significant difference between  $\tau_d$  obtained for  $Z = 0.02$  models calculated using the most recent opacities, and the electron scattering cases. This highlights an important contribution of opacity to the instability of very massive stars with solar metallicity. Indeed, the driving zones in the  $Z = 0.02$  ZAMS models with  $M \geq 200 M_\odot$  are located at  $\log T \sim 5.2 - 5.3$  K and are associated with a sharp peak of the opacity in this region due to the contribution of heavy elements (Iglesias & Rogers 1996). For  $120 M_\odot$  with  $Z \geq 0.01$ , our results are in agreement with the analysis of Glatzel & Kiriakidis (1993): the driving for the first overtone is due to the  $\kappa$ -mechanism whereas for the fundamental mode, both the  $\epsilon$ - and the  $\kappa$ -mechanisms contribute to the driving.

As  $Z$  decreases, we find a transition between nuclear-driven pulsation and opacity-driven pulsation (i.e., the  $\epsilon$ - and  $\kappa$ -mechanisms). The  $\epsilon$ -mechanism is dominant for  $Z \lesssim 2 \times 10^{-4}$  and the  $\kappa$ -mechanism dominates for  $Z \gtrsim 2 \times 10^{-3}$ , for the mass range of interest. The increase of  $\tau_d$  as  $Z$  decreases for  $Z \lesssim 2 \times 10^{-4}$  is partly due to the different temperature dependence of the nuclear energy generation from the CNO cycle. As shown in Table 1, central hydrogen burning proceeds at higher  $T$  for decreasing  $Z$ .

Locally, the temperature dependence of the specific nuclear energy generation rate,  $\epsilon_{\text{nuc}}$ , depends on temperature as  $\epsilon_{\text{nuc}} \propto T^\nu$ , where  $\nu := \partial \ln \epsilon_{\text{nuc}} / \partial \ln T$ . Since the temperature sensitivity,  $\nu$ , of hydrogen burning by the CNO-cycle decreases with increasing temperature (e.g., Kippenhahn & Weigert, 1992, Figure 18.8) the metal-rich stars have a stronger sensitivity than the metal poor stars. We find  $\nu \sim 10$  for  $Z = 0$  and  $\nu$  increases with  $Z$  up to  $\sim 14$  for  $Z = 0.02$  in the  $120 M_\odot$  star. Analytically  $\nu$  can be computed from  $\nu = (\tau - 2)/3$  where

$$\tau = 4.248 \left( Z_1^2 Z_2^2 \frac{A_1 A_2}{A_1 + A_2} / T_9 \right)^{1/3}. \quad (1)$$

$A_1, A_2, Z_1, Z_2$  are mass number and charge number of the two input nuclei, and  $T_9$  is the temperature in  $10^9$  K (Clayton 1968). For  $^{14}\text{N}(p, \gamma)$ ,  $\nu = 14$  at  $T_9 = 0.04$  and  $\nu = 10$  at  $T_9 = 0.1$ , in agreement with the values obtained above.

Since the driving of pulsations due to the  $\epsilon$ -mechanism depends directly on  $\nu$  with  $W \propto \nu$ , it is larger in metal-rich than in metal-free stars, contributing to the decrease of  $\tau_d = 1/K \propto$

$1/W$  as  $Z$  increases. Another contribution to  $\tau_d$  comes from the total pulsation energy  $E_{\text{puls}} \propto 1/P^2$ , since  $K \propto 1/E_{\text{puls}} \propto P^2$  (see next section Eqs. (3) and (4)) and  $P$  increases with  $Z$ , as mentioned above. As long as the contribution of metals to the opacity is negligible, this explains why  $\tau_d = 1/K \propto 1/P^2 W$  decreases as  $Z$  increases. Once the  $\kappa$ -mechanism operates in the envelope, it yields a dramatic increase of  $W$  and significantly smaller  $\tau_d$ , by up to six orders of magnitude (see Table 1).

#### 4. MASS LOSS RATES

In order to derive a realistic mass loss rate, non-linear calculations would be required to determine the pulsation amplitudes and dissipation due to shock wave formation. Non-linear calculations have been performed for the solar metallicity case by various authors (Appenzeller 1970ab; Ziebarth 1970; Papaloizou 1973a; Talbot 1971ab) who, unfortunately, give different results. Appenzeller (1970ab) finds an upper limit  $\dot{M} = 5 \times 10^{-5} M_{\odot} \text{yr}^{-1}$  for a  $130 M_{\odot}$  star and  $\dot{M} = 5 \times 10^{-4} M_{\odot} \text{yr}^{-1}$  for a  $270 M_{\odot}$  star, whereas Papaloizou (1973b) finds stronger dissipation effects and mass loss rates less than  $10^{-6} M_{\odot} \text{yr}^{-1}$  for similar masses.

Since the dissipation effects in Appenzeller (1970ab) may be underestimated compared to other studies, yielding larger mass loss rates, we used his results to derive an upper limit for  $\dot{M}$  for the  $Z = 0$  models. Appenzeller found that when the velocity amplitude at the surface approached the sound speed, mass loss sets in. An upper limit of the mass loss rate came from assuming that the entire rate of gain of pulsation energy,  $L_{\text{puls}}$ , was used to accelerate the matter to escape velocity,  $v_{\text{esc}} = \sqrt{2GM/R}$ . Thus one has:

$$\frac{\dot{M}}{2} v_{\text{esc}}^2 = L_{\text{puls}}. \quad (2)$$

$L_{\text{puls}}$  can be estimated from the total pulsation energy  $E_{\text{puls}}$ , averaged over one period, and the stability coefficient,  $K$  (see Cox 1980), with

$$L_{\text{puls}} = 2KE_{\text{puls}}, \quad (3)$$

where

$$E_{\text{puls}} = \frac{1}{2} \left( \frac{2\pi}{P} \right)^2 \int_0^M \delta r^2 dM. \quad (4)$$

Since the relative pulsation amplitude,  $\delta r / \delta r_{\text{surf}}$ , is given by our linear stability analysis,  $\delta r_{\text{surf}}$  and thus  $E_{\text{puls}}$  are estimated by assuming, like Appenzeller (1970ab), that the surface velocity amplitude reaches the sound speed,  $c_{\text{sound}}$ , i.e.:

$$\frac{2\pi}{P} \delta r_{\text{surf}} = c_{\text{sound}}. \quad (5)$$

For the zero metallicity stars from  $120$  to  $500 M_{\odot}$ ,  $c_{\text{sound}}$  is typically  $(1 - 1.6) \times 10^7 \text{cm s}^{-1}$ . The resulting energy,  $E_{\text{puls}}$ , and mass loss rates for the  $Z = 0$  models on the ZAMS are given in Table 3. Results are also given for the  $120 M_{\odot}$  star with  $Z = 0.02$  and pure electron scattering opacity. Our upper limit for  $\dot{M}$  in this case is in good agreement with Appenzeller's value of  $5 \times 10^{-5} M_{\odot} \text{yr}^{-1}$  for similar masses. A crude upper limit for the total mass lost  $\Delta M$  during hydrogen burning is derived assuming that mass loss proceeds at constant rate as long as the star remains unstable, i.e., during the time  $\tau_{\text{stable}}$  (see Table 3). In any case,  $\Delta M$  does not exceed 5 % of the total mass for zero-metal stars. Note that this estimate neglects the time required for the pulsation amplitude to grow to the value  $\delta r_{\text{surf}}$  characterizing the beginning of mass loss (Eq. (5)). Given the non negligible value of  $\tau_d$  compared to  $\tau_{\text{stable}}$  (see Table 1), this time may

be significant for the  $120 M_{\odot}$  star. In fact, this star may never encounter pulsationally driven mass loss. Moreover, since the stars stabilize as soon as they evolve away from the ZAMS (see Sect. 3.1.2) with decreasing  $K$  (see Fig. 4), one can expect decreasing  $\dot{M}$  along the main sequence, and thus even smaller values for  $\Delta M$ . We thus find that even for  $500 M_{\odot}$  star, pulsations do not lead to significant mass loss on the main sequence.

For post-main sequence evolution, as found in Sect. 3.1.2, only stars with initial masses of  $\gtrsim 300 M_{\odot}$  become unstable again during helium burning and can undergo another phase of mass loss. Any estimate of mass loss is hampered by the lack of non-linear calculations during these late phases of evolution. Moreover, as the star evolves toward low effective temperature and eventually becomes a red supergiant, it develops a deep convective envelope, the opposite of main sequence stars. This adds additional difficulty to any derivation of  $\dot{M}$  since convection can have an important contribution to the damping or driving of the pulsation in this case.

#### 5. DISCUSSION AND CONCLUSIONS

Our analysis has shown that even though metal-free stars with  $120 M_{\odot} \leq M \leq 500 M_{\odot}$  are radially unstable on the main sequence (like their metal-enriched counterparts), the efficiency of the  $\epsilon$ -mechanism is reduced because of the hotter central  $T$  and more compact structure. Consequently, the  $e$ -folding times characterizing the growth of amplitudes are much longer. After burning some hydrogen, the stars stabilize (Table 2).

In order to know the effects of such oscillations and accurately estimate the resulting pulsationally driven wind, non-linear calculations would be required. We have not done those and have only estimated the mass loss using simple arguments based upon previous non-linear calculations. Adopting the approach of Appenzeller (1970ab) that the mass loss can be derived from the energy gain rate of the pulsation when its surface velocity reaches the local velocity of sound at least gives a quantitative result which is a reasonable upper limit (Sect. 4). For the  $120 M_{\odot}$  star we find negligible mass loss during the central hydrogen burning phase. The integrated mass loss during central hydrogen burning of about  $2.5 M_{\odot}$  for a  $200 M_{\odot}$  star increases to about  $25 M_{\odot}$  for the  $500 M_{\odot}$  star - less than 5 % of its initial mass.

We also note that Papaloizou (1973b) disagrees with the results of Appenzeller (1970a) and finds an important limitation of the pulsation amplitude, which cannot drive any mass loss. If this is the case for the solar metallicity stars, it is even more so for metal-free stars. Therefore we conclude that mass loss during central hydrogen burning remains unimportant for the evolution of all the  $Z=0$  stars investigated (Table 3).

Finally, it is worth noting that the strong instability found at the end of core helium burning for  $M \geq 300 M_{\odot}$  could have important consequences. What exactly happens depends on the remaining time before collapse (only a few 10 kyr for the 300 and  $500 M_{\odot}$  stars investigated here) and, especially, on the strength of the mass loss rates achieved in these pulsating giant stars with convective envelopes. This is an important issue regarding the gamma-ray burst scenario suggested by Fryer et al. (2000) and needs further investigation.

From our estimates of the mass loss rates we conclude that primordial very massive stars of  $\lesssim 500 M_{\odot}$  (but over  $100 M_{\odot}$ ) reach core collapse with helium cores massive enough to encounter the pair creation instability. Single stars probably

TABLE 1  
PROPERTIES OF ZAMS MODELS AS A FUNCTION OF MASS AND METALLICITY.

| $M (M_{\odot})$ | $Z$                  | $T_{\text{eff}} (\text{kK})$ | $R (R_{\odot})$ | $T_c (10^8 \text{ K})$ | $P (\text{d})$ | $\tau_d (\text{yr})$                   |
|-----------------|----------------------|------------------------------|-----------------|------------------------|----------------|--|
| 120             | 0                    | 99.2                         | 4.6             | 1.38                   | 0.064          | $1.4 \times 10^4$                      |
|                 | $2 \times 10^{-6}$   | 72.9                         | 8.2             | 0.74                   | 0.16           | $5.6 \times 10^3$                      |
|                 | $2 \times 10^{-5}$   | 67.1                         | 9.6             | 0.63                   | 0.20           | $4.2 \times 10^3$                      |
|                 | $2 \times 10^{-4}$   | 62.6                         | 11.0            | 0.55                   | 0.25           | $3.7 \times 10^3$                      |
|                 | 0.01                 | 53.3                         | 15.2            | 0.45                   | 0.34 (0.16)    | $4.6 \times 10^3 (2.3 \times 10^1)$    |
|                 | 0.02                 | 48.9                         | 18.4            | 0.44                   | 0.36 (0.26)    | $1.9 \times 10^2 (1.4 \times 10^{-3})$ |
|                 | 0.02 ( $e^-$ scatt.) | 67.1                         | 13.2            | 0.45                   | 0.34           | $7.8 \times 10^2$                      |
| 200             | 0                    | 104.2                        | 6.0             | 1.43                   | 0.083          | $3.7 \times 10^3$                      |
|                 | 0.02                 | 44.9                         | 32.1            | 0.46                   | 0.76           | $1.3 \times 10^{-3}$                   |
|                 | 0.02 ( $e^-$ scatt.) | 70.5                         | 17.5            | 0.47                   | 0.45           | $5.3 \times 10^2$                      |
| 300             | 0                    | 107.0                        | 7.6             | 1.47                   | 0.10           | $2.6 \times 10^3$                      |
|                 | $2 \times 10^{-4}$   | 68.1                         | 18.2            | 0.60                   | 0.39           | $1.3 \times 10^3$                      |
|                 | 0.02                 | 39.8                         | 54.1            | 0.47                   | 1.79           | $2.1 \times 10^{-3}$                   |
|                 | 0.02 ( $e^-$ scatt.) | 72.5                         | 22.0            | 0.48                   | 0.55           | $4.3 \times 10^2$                      |
| 500             | 0                    | 109.2                        | 10.0            | 1.51                   | 0.13           | $2.0 \times 10^3$                      |

NOTE.— The pulsation period and  $e$ -folding time are given for the fundamental mode. Only for  $120 M_{\odot}$  with  $Z \geq 0.01$  the fundamental mode and first overtone (in parentheses) are both unstable. For  $Z = 0.02$ , results based on models calculated with pure electron scattering opacity ( $e^-$  scatt.) are also given.

TABLE 2  
PROPERTIES OF  $Z = 0$  STARS DURING CORE HYDROGEN BURNING.

| $M (M_{\odot})$ | $\tau_H (\text{Myr})$ | $\tau_{\text{stable}} (\text{Myr})$ | $Y_c (\%)$ | $A_{\text{max}}$ |
|-----------------|-----------------------|-------------------------------------|------------|------------------|
| 120             | 2.35                  | 0.25                                | 69         | 10               |
| 200             | 2.15                  | 0.52                                | 58         | 69               |
| 300             | 1.94                  | 0.63                                | 51         | 130              |
| 500             | 1.74                  | 0.70                                | 46         | 216              |
| 120es           | 1.74                  | 0.97                                | 33         | 1091             |

NOTE.— The table gives the initial mass  $M$ , the total hydrogen-burning lifetime of the star  $\tau_H$ , the age at which the star becomes stable  $\tau_{\text{stable}}$ , the central hydrogen mass fraction at this time  $Y_c$  (initial value is 76 %), and the number of  $e$ -folds an initial pulsation has grown since the ZAMS by then,  $A_{\text{max}} = \int_0^{\tau_{\text{stable}}} K(t) dt$ .

TABLE 3  
MASS LOSS ESTIMATES OF STARS AT ZAMS.

| $M (M_{\odot})$ | $Z$                  | $E_{\text{puls}} (10^{48} \text{ erg})$ | $\dot{M} (M_{\odot} \text{ yr}^{-1})$ | $\Delta M (M_{\odot})$ |
|-----------------|----------------------|---|---------------------------------------|------------------------|
| 120             | 0                    | 0.5                                     | $7.5 \times 10^{-7}$                  | 0.2                    |
| 200             | 0                    | 1                                       | $5 \times 10^{-6}$                    | 2.5                    |
| 300             | 0                    | 2.5                                     | $1.3 \times 10^{-5}$                  | 8.5                    |
| 500             | 0                    | 6                                       | $3.5 \times 10^{-5}$                  | 24.5                   |
| 120             | 0.02 ( $e^-$ scatt.) | 0.2                                     | $1.7 \times 10^{-5}$                  | 17                     |

NOTE.— The table gives the initial mass,  $M$ , metallicity,  $Z$ , pulsation energy,  $E_{\text{puls}}$ , mass loss rate at the ZAMS, and an estimate of the total mass lost during the time the stars are unstable ( $\tau_{\text{stable}}$ , see Table 2) during central hydrogen burning, i.e.,  $\Delta M = \dot{M} \tau_{\text{stable}}$ . The results for  $120 M_{\odot}$ ,  $Z = 0.02$  and pure electron scattering opacity is also given.

do not lose their hydrogen envelope for initial masses of  $\lesssim 300 M_{\odot}$ . The nucleosynthetic yields of these stars can be important for the chemical evolution of the early universe, as they may eject up to  $60 M_{\odot}$  of  $^{56}\text{Ni}$  for a  $\approx 250 M_{\odot}$  star (Heger & Woosley 2000). Still heavier stars make black holes (Bond, Arnett & Carr 1984). Extrapolating from our results, we speculate that stars of  $\gtrsim 1000 M_{\odot}$  might experience such strong mass loss that they end their lives as smaller objects. But clearly the stability of these massive “first stars” is a subject worthy of additional exploration beyond the first linear stability analysis presented here.

We are grateful to Gilles Chabrier for many valuable discussion. IB thanks the Astronomy Departments of University of California at Berkeley and Santa-Cruz for hospitality during the completion of this work. This research was supported, in part, by Prime Contract No. W-7405-ENG-48 between The Regents of the University of California and the United States Department of Energy, the National Science Foundation (AST 97-31569, INT-9726315), and the Alexander von Humboldt-Stiftung (FLF-1065004).

## REFERENCES

- Abel, T., Anninos, P., Norman, M.L., Zhang, Y. 1998, *ApJ*, 508, 518  
 Abel, T., Bryan, G. L., & Norman, M. L. 2000, *ApJ*, in press, astro-ph/0002135  
 Aizenman, M.L., Hansen, C.J., Ross, R.R. 1975, 201, 387  
 Alibert, Y., Baraffe, I., Hauschildt, P.H., Allard, F. 1999, *A&A*, 344, 551  
 Appenzeller, I. 1970a, *A&A*, 5, 355  
 Appenzeller, I. 1970b, *A&A*, 9, 216  
 Baraffe, I., El Eid, M.F. 1991, *A&A*, 245, 548  
 Baraffe, I., Alibert, Y., Méra, D., Chabrier, G., Beaulieu, J-P. 1998, *ApJ*, 499, L205  
 Bond, J. R., Arnett, W. D., & Carr, B. J. 1984, *ApJ*, 280, 825  
 Bromm, V., Coppi, P.S., Larson, R.B. 1999, *ApJ*, 527, L5  
 Buchmann, L. 1996, *ApJL*, 468, L127  
 Caughlan, G.R., Fowler, W.A. 1988, *Atom. Data and Nucl. Data Tables*, 40, 283  
 Clayton, D., 1968, *Principles of Stellar Evolution and Nucleosynthesis*, University of Chicago Press.  
 Cox, J.P. 1980, *Theory of Stellar Pulsations*, Princeton University Press, p. 114  
 Cox, A.N., Cahn, J.H. 1988, *ApJ*, 326, 804  
 Ezer, D., & Cameron, A. G. W. 1971, *Ap&SS*, 14, 399  
 Fryer, C., Woosley, S.E., Heger, A. 2000, *ApJ*, submitted, astro-ph/0007176  
 Glatzel, W., El Eid, M. F., & Fricke, K. J. 1985, *A&A*, 149, 413  
 Glatzel, W., Kiriakidis, M. 1993, *MNRAS*, 262, 85  
 Hartquist, T. W., & Cameron, A. G. W. 1977, *Ap&SS*, 48, 145.  
 Heger, A. 1998, PhD Thesis, University of Munich, Germany  
 Heger, A., Jeannin, L., Langer, N., Baraffe, I. 1997, *A&A*, 327, 224  
 Heger, A., & Langer, N. 2000, *ApJ*, in press  
 Heger, A., Langer, N., & Woosley, S. E. 2000a, *ApJ*, 528, 368  
 Heger, A., Woosley, S. E. 2000, *ApJ*, in preparation  
 Iglesias, C.A., Rogers, F.J. 1996, *ApJ*, 464, 943  
 Kippenhahn, R., and Weigert, A., 1992, “Stellar Structure and Evolution”, 2<sup>nd</sup> ed., Springer-Verlag, Berlin  
 Kiriakidis, M., Fricke, K. J., Glatzel, W. 1993, *MNRAS*, 264, 50  
 Kudritzki, R.-P. 2000, in *The First Stars*, eds. A. Weiss, T. Abel and V. Hill, Proceedings of the 2nd ESO/MPA conference, Springer, Heidelberg, in press  
 Langer, N., Kiriakidis, M., El Eid, M. F., Fricke, K. J., Weiss, A. 1998, *A&A*, 192, 177  
 Larson, R.B. 1999, to be published in the ESA Special Publications Series (SP-445), edited by F. Favata, A. A. Kaas, and A. Wilson, astro-ph/9912539  
 Ledoux, P. 1941, *ApJ*, 94, 537  
 Lee, U. 1985, *PASJ*, 37, L261  
 Maeder, A. 1985, *A&A*, 147, 300  
 Meynet, G., Maeder, A., Schaller, G., Schaerer, D., and Charbonnel, C. 1994, *A&AS*, 103, 97  
 Ostriker, J.P., Gnedin, N.Y. 1996, *ApJ*, 472, L63  
 Palla, F., Salpeter, E.E., Stahler, S.W. 1983, *ApJ*, 271, 632  
 Papaloizou, J.C.B. 1973a, *MNRAS*, 162, 143  
 Papaloizou, J.C.B. 1973b, *MNRAS*, 162, 169  
 Schwarzschild, M., & Spitzer, L. 1953, *Observatory*, 73, 77.  
 Schwarzschild, M., & Härm, R. 1959, *ApJ*, 129, 637  
 Silk, J. 1983, *MNRAS*, 205, 705  
 Stothers, R. 1992, *ApJ*, 392, 706  
 Stothers, R., Simon, N.R. 1968, *ApJ*, 152, 233  
 Talbot, R.J., 1971a, *ApJ*, 163, 17  
 Talbot, R.J., 1971b, *ApJ*, 165, 121  
 Unno W., Osaki Y., Ando, H., Saio, H., Shibahashi, H. 1989, *Nonradial oscillations of stars*, Univ. of Tokyo Press.  
 Yoneyama, T. 1972, *PASJ*, 24, 87  
 Ziebarth, K. E. 1970, *ApJ*, 162, 947